


Stochastic line integrals and stream functions as metrics of irreversibility and heat transfer

Stephen Teitsworth*

*Department of Physics, Duke University, Box 90305, Durham, North Carolina 27708-0305, USA*John C. Neu *Department of Mathematics, University of California, Berkeley, Berkeley, California 94720-3840, USA*

(Received 31 March 2022; accepted 9 August 2022; published 24 August 2022)

Stochastic line integrals are presented as a useful metric for quantitatively characterizing irreversibility and detailed balance violation in noise-driven dynamical systems. A particular realization is the stochastic area, recently studied in coupled electrical circuits. Here we provide a general framework for understanding properties of stochastic line integrals and clarify their implementation for experiments and simulations. For two-dimensional systems, stochastic line integrals can be expressed in terms of a stream function, the sign of which determines the orientation of nonequilibrium steady-state probability currents. Theoretical results are supported by numerical studies of an overdamped two-dimensional mass-spring system driven out of equilibrium. Additionally, the stream function permits analytical understanding of the scaling dependence of stochastic area growth rate on key parameters such as the noise strength for both linear and nonlinear springs.

DOI: [10.1103/PhysRevE.106.024124](https://doi.org/10.1103/PhysRevE.106.024124)**I. INTRODUCTION**

Understanding and quantitatively characterizing irreversibility and related phenomena is a central task in the study of noise-driven nonequilibrium systems. Such systems are of interest throughout the natural sciences with examples in diverse fields such as biophysics [1,2], climate dynamics [3,4], optically levitated nanoparticles [5–7], and electronic transport systems and circuits [8–10]. Well-known approaches for understanding nonequilibrium behavior focus on characterizing the dynamics with physically inspired metrics such as entropy production and heat transfer [2,11,12]. One advantage of such techniques is that they connect directly to the nonequilibrium behavior of the underlying system, e.g., heat transfer from a hot mass to a cold mass in a coupled mass-spring system [12,13]. However, for many systems of interest, the nonequilibrium dynamics is not directly determined by thermal gradients [1,14] and the implementation of such metrics may not be straightforward. For example, biophysical systems such as beating flagella and cilia are typically driven by chemical (metabolic and enzymatic) processes [1], while nonlinear electronic circuits may be driven by external voltage noise sources as well as internal nonthermal sources (e.g., shot noise) associated with nonlinear elements such as tunnel diodes [10]. For such systems, measured time series oftentimes do not have a direct or obvious connection to heat transport or entropy production, and the question naturally arises how to best quantify nonequilibrium dynamical behavior.

This has motivated the introduction of a variety of theoretical and empirical metrics to characterize and quan-

tify the extent of nonequilibrium behavior. Such metrics include probability angular momentum [4,15,16], cycling frequencies [17], dissipation rate inference schemes [14,18], information-theoretic methods [19], and stochastic area [20]. One advantage of these metrics is that they can often be computed directly from experimental data time series and without knowledge of a detailed underlying model. In this paper we introduce and explore two such metrics: (i) the stochastic line integral (SLI), which is a generalization of the recently introduced stochastic area [20], and (ii) a stochastic stream function applicable to two-dimensional systems in steady state.

To frame the discussion, it is useful to start by recalling a key aspect of Brownian motion as a prototype for a large class of stochastic dynamical systems: a small number of macroscopic degrees of freedom are distinguished from a great multitude of others called microscopic by the nature of couplings. The couplings of any one microscopic degree of freedom to the macroscopic degrees are small, but the collective action of the microscopic degrees upon the macroscopic degrees is comparable to the couplings of the macroscopic degrees among themselves. This being so, individual identities of the microscopic degrees of freedom are not retained. Their collective actions upon the macroscopic degrees of freedom are modeled by random fluctuations and by dissipation. As a concrete example, we can imagine a mechanical assembly immersed in a fluid, its movements stimulated by individual impacts of fluid particles, and inhibited by drag. An example with two masses coupled by springs, which we analyze in greater detail below, is depicted in Fig. 1. Here we envision that the mass on the left with position x_1 is stochastically driven by thermal fluctuations of temperature T_1 while moving in the deterministic potential energy produced by the attached coupling springs and similarly for the mass on the right at

*teitso@phy.duke.edu

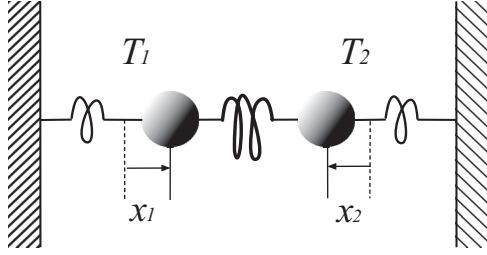


FIG. 1. Linear mass-spring network of two Brownian particles (labeled with coordinates x_1 and x_2) and driven by thermal fluctuations at respective temperatures T_1 and T_2 .

position x_2 , which is driven by thermal fluctuations of temperature T_2 .

In the overdamped limit which neglects inertia, we model the statistics of the macroscopic degrees of freedom by an Itô stochastic differential equation (SDE) [21]

$$d\mathbf{x}(t) = \mathbf{u}(\mathbf{x}(t))dt + \sigma d\mathbf{W}(t) + O((dt)^{3/2}). \quad (1)$$

Here $\mathbf{x}(t)$ is the time series of the state vector in \mathbb{R}^n , dt is the time step, and $d\mathbf{x}(t)$ is the forward difference

$$d\mathbf{x}(t) := \mathbf{x}(t + dt) - \mathbf{x}(t). \quad (2)$$

The vector field $\mathbf{u}(\mathbf{x})$ is the deterministic flow and $d\mathbf{W}(t)$ denotes the forward difference of the vector Wiener process with statistics [21]

$$\langle dW_i(t) \rangle = 0, \quad \langle dW_k(t)dW_l(t) \rangle = \delta_{kl}dt. \quad (3)$$

Here σ is a constant noise tensor which determines the linear combinations of the dW_i which induce fluctuations in each component of $d\mathbf{x}$. On the account of (3), we think of $d\mathbf{W}$ as formally $O(\sqrt{dt})$.

The structure of the paper is as follows. In Sec. II we examine the projection of statistics in the full Hamiltonian phase space with all the degrees of freedom, including the microscopic, onto a reduced statistics which sees only the macroscopic degrees of freedom.¹ Elementary analysis shows that the projected statistics is characterized by a continuity equation for $\rho(\mathbf{x}, t)$, the marginal of the phase-space probability density. This marginal has an associated probability current $\mathbf{J}(\mathbf{x}, t)$. There is no *a priori* determination of this “exact” probability current as a simple functional of the reduced probability density ρ . Nevertheless, we show that microscopic reversibility [22] implies that \mathbf{J} vanishes identically for Hamiltonian systems that are closed with stationary probability density. Conversely, nonvanishing of \mathbf{J} associated with macroscopic irreversibility is possible for closed systems when the full probability density is not strictly stationary.

¹This also provides helpful insight when we apply metrics such as the stochastic line integral directly to real experimental data collected from high-dimensional systems. The process of experimentally measuring only a few macroscopic variables is qualitatively related to the theoretical process of projecting from a high-dimensional microscopic model (e.g., with the number of degrees of freedom of order of Avogadro’s number) to SDE models described by (1).

In Sec. III we examine line integrals over trajectories on macroscopic state space projected from the full Hamiltonian phase space. They are useful detectors of irreversibility as pointed out in recent theoretical and experimental work that focused on one particular realization called stochastic area [9,20]. To develop a general definition, let

$$C(t): \mathbf{x} = \mathbf{x}(t'), \quad 0 < t' < t, \quad (4)$$

be such a trajectory. Form the line integral

$$G(t) := \int_{C(t)} g_i dx_i = \int_0^t g_i(\mathbf{x}(t')) \dot{x}_i(t') dt', \quad (5)$$

where g_i is an arbitrary vector-valued function of \mathbf{x} and a summation convention is used, i.e., repeated Cartesian indices are summed over. (For the special case of stochastic area, one chooses $g_1 = -\frac{x_2}{2}$ and $g_2 = \frac{x_1}{2}$.) We show that the ensemble average generally satisfies

$$\frac{d}{dt} \langle G \rangle(t) := \frac{d}{dt} \left\langle \int_{C(t)} g_i dx_i \right\rangle = \int_{\mathbb{R}^n} g_i(\mathbf{x}) J_i(\mathbf{x}, t) d\mathbf{x}, \quad (6)$$

so the nonvanishing of ensemble-averaged line integrals indicates irreversibility. In the general nonstationary case we expect $d\langle G \rangle/dt$ to have explicit time dependence. However, in the important case where the probability current J_i is stationary or quasistationary, $d\langle G \rangle/dt$ will be time independent.

The statistics on the macroscopic state space governed by the stochastic ordinary differential equation (ODE) approximates the exact statistics based upon projection from the full Hamiltonian phase space. In Sec. IV we examine the analog of the stochastic line integral formula (6) within the statistics governed by the SDE (1). We focus on those systems where the exact probability current \mathbf{J} can be reasonably approximated by a Fokker-Planck probability current [21],

$$\mathbf{j}(\mathbf{x}, t) := \mathbf{u}(\mathbf{x})\rho - D\nabla\rho. \quad (7)$$

Here $\rho(\mathbf{x}, t)$ denotes the reduced probability density over the macroscopic position variables and

$$D := \frac{1}{2} \sigma \sigma^T \quad (8)$$

is the diffusion tensor induced by the noise tensor σ in (1). The Fokker-Planck expression works well for a wide variety of experimentally relevant noise-driven systems. Examples of recent interest include electronic circuits driven by thermal noise [23] and filament dynamics in active biological networks driven by nonequilibrium noise [2,24].

We propose and analyze two definitions of stochastic line integral closely related to the Stratonovich stochastic integral [21,25] and show their equivalence. For both we find that the stochastic line integral formula (6) holds with the Fokker-Planck probability current \mathbf{j} in place of \mathbf{J} .

To illustrate the general points in earlier sections and to show connections of stochastic line integrals with physically relevant concepts such as heat transfer, Sec. V examines the overdamped statistics of a well-established paradigm system of two coupled Brownian particles in heat baths of temperatures T_1 and T_2 (cf. Fig. 1). Heat transfer between the baths is analyzed for the case of linear coupling, starting from its characterization by a specific type of the stochastic line integral,

the stochastic area [20]. For two-dimensional systems, simulations may be complemented by a theoretical quantification of heat transfer in terms of the stream function for the stationary probability current. We show how stochastic line integrals may generally be expressed as relatively simple integrals of the stream function and how this allows us to analytically infer physically significant properties such as heat transfer rate. Finally, in Sec. VI we discern the effects of nonlinearity by studying the scaling dependence of time rate of change in stochastic area versus noise amplitude. In particular, we show analytically that hard spring nonlinearity inhibits heat transfer relative to a linear system, as the temperature difference increases.

II. PROJECTION OF HAMILTONIAN PHASE SPACE ONTO MACROSCOPIC VARIABLES

To understand the broad applicability of SLIs it is useful to consider how they follow from a microscopic perspective. Here we focus on high-dimensional closed classical Hamiltonian systems and carry out projections [26]. However, the motivation to do this is not purely formal since, for a wide range of experimental noise-driven nonequilibrium systems, one can in principle associate a set of classical Hamiltonians provided there are enough degrees of freedom and the functional form of the Hamiltonian H is appropriately chosen. Equivalently, we expect that a classical experimental system can be simulated with arbitrary accuracy by a reversible classical computer which in turn can be associated with a classical Hamiltonian flow [27].

Let \mathbf{X} and \mathbf{P} be N -vectors of coordinates and momenta of the full Hamiltonian dynamics. We assume that the Hamiltonian has a structure such that the first $n \ll N$ components of \mathbf{X} can be identified as macroscopic coordinates.² In that case, the projection of the trajectory $(\mathbf{X}_{(t)}^{(i)}, \mathbf{P}_{(t)}^{(i)})$ in $2N$ -dimensional phase space onto the space of macroscopic coordinates is

$$\mathbf{x} := \begin{pmatrix} X_1(t) \\ \vdots \\ X_n(t) \end{pmatrix}.$$

For convenience of discussion, we define all of the remaining microscopic coordinates by

$$\tilde{\mathbf{X}} := \begin{pmatrix} X_{n+1}(t) \\ \vdots \\ X_N(t) \end{pmatrix}.$$

Figure 2 visualizes the projection from the Hamiltonian phase space onto the state space of macroscopic coordinates. Any ensemble of trajectories on the full phase space is transported by the Hamiltonian flow, so the full probability density $f(\mathbf{X}, \mathbf{P}, t)$ satisfies a continuity condition or, equivalently, the

²More generally, in cases where the Hamiltonian does not have this structure, we note that it may sometimes be possible to bring it into a form that clearly separates macroscopic and microscopic coordinates via suitable canonical transformation.

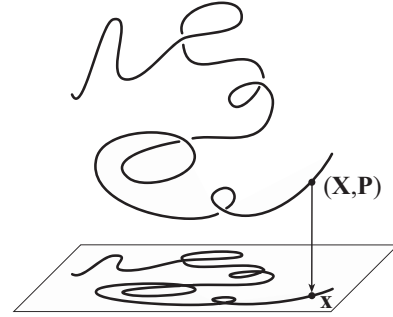


FIG. 2. Depiction of the projection from full phase space onto the space of macroscopic states.

classical Liouville equation [26]

$$\frac{\partial}{\partial t} f + \frac{\partial}{\partial X_i} \left(\frac{\partial H}{\partial P_i} f \right) - \frac{\partial}{\partial P_i} \left(\frac{\partial H}{\partial X_i} f \right) = 0. \quad (9)$$

Here $H(\mathbf{X}, \mathbf{P})$ is the (autonomous) Hamiltonian. Given an ensemble of trajectories on the full phase space, we examine its projection onto the space of macroscopic coordinates. The probability density of the projected ensemble is

$$\rho(\mathbf{x}, t) := \int_{\mathbb{R}^{N-n}} d\tilde{\mathbf{X}} \left(\int_{\mathbb{R}^N} d\mathbf{P} f \right). \quad (10)$$

Here $d\tilde{\mathbf{X}} := dX_{n+1} \cdots dX_N$ is the volume element of microscopic coordinates. By integrating (9) over *all* momenta and microscopic coordinates, we arrive at the projection of the continuity equation onto the space of macroscopic coordinates,

$$\frac{\partial}{\partial t} \rho + \sum_{i=1}^n \frac{\partial}{\partial X_i} \int_{\mathbb{R}^{N-n}} d\tilde{\mathbf{X}} \left(\int_{\mathbb{R}^N} d\mathbf{P} \frac{\partial H}{\partial P_i} f \right) = 0. \quad (11)$$

Here we recognize

$$J_i(\mathbf{x}, t) := \int_{\mathbb{R}^{N-n}} d\tilde{\mathbf{X}} \left(\int_{\mathbb{R}^N} d\mathbf{P} \frac{\partial H}{\partial P_i} f \right) \quad (12)$$

for $i = 1, \dots, n$ as the components of projected probability current in the space of macroscopic coordinates.

As expected for generic Hamiltonian flows, we assume that $H(\mathbf{X}, \mathbf{P})$ is even in the momenta [26]. If $(\mathbf{X}_{(t)}^{(i)}, \mathbf{P}_{(t)}^{(i)})$ is a realizable phase-space trajectory, then so is its time reversal $(\mathbf{X}_{(-t)}^{(i)}, -\mathbf{P}_{(-t)}^{(i)})$. Following Onsager [22], we assume an equilibrium ensemble in phase space which is stationary and invariant under interchange of all trajectories with their time reversals. Let $f_s(\mathbf{X}, \mathbf{P})$ be the stationary probability density of the original ensemble. At $t = 0$, swap every trajectory for its time reversal. The probability density after the swap is $f_s(\mathbf{X}, -\mathbf{P})$. Then, due to the aforementioned invariance, we must have $f_s(\mathbf{X}, \mathbf{P}) = f_s(\mathbf{X}, -\mathbf{P})$ so that f_s is even in \mathbf{P} . Given the even symmetries of H and f_s in the momenta, we see that the projected probability current (12) must vanish for all \mathbf{x} . We anticipate that equilibrium modeled by the stochastic ODE (1) should likewise have zero probability current. In the context of overdamped stochastic ODEs such as (1), this property is called detailed balance [28,29]. It is equivalent to microscopic

reversibility because the forward direction of time cannot be inferred from the stationary reduced statistics.

Here we are interested in systems where the reduced statistics of macroscopic variables is irreversible, i.e., nonvanishing projected probability current. What does irreversibility of reduced statistics mean in the context of a much larger whole which is assumed to be reversible and closed? An illustrative scenario is the situation of two heat baths, each with many degrees of freedom, coupled to one another via a few macroscopic degrees of freedom. Figure 1 visualizes a mechanical example which has been studied extensively as a paradigmatic nonequilibrium system that breaks detailed balance (see, e.g., [11,12,14]). A mass-spring system consists of two Brownian particles moving in baths at different temperatures. They are trapped by restoring forces and coupled to each other by a linear spring. A temperature difference between the baths drives heat transfer from hot to cold. Strictly speaking, the statistics on the full phase space (including all the microscopic degrees of freedom) cannot be stationary. Nevertheless, we anticipate that stationary reduced statistics representing the steady heat transfer is achieved asymptotically as the heat capacities of the baths become very large. This means that the projected statistics of the full Hamiltonian system must settle into a quasistationary state for a very long time, longer than the duration of any measurement. Conversely, the lower bound on the timescale for quasistationary behavior is limited by the transients to decay from typical arbitrary initial conditions to the quasistationary state, a timescale that is, relatively speaking, many of orders of magnitude smaller. For overdamped systems, this decay time is typically determined by linearizing the deterministic part of the flow in the SDE.³

III. STOCHASTIC LINE INTEGRALS IN FULL PHASE SPACE

In this section we show generally how stochastic line integrals can be written in terms of the projected probability currents. Let

$$\frac{d}{dt}\langle G \rangle := \frac{d}{dt} \left\langle \int_{C(t)} g_i dx_i \right\rangle = \langle g_i(\mathbf{x}) \dot{x}_i \rangle \quad (13)$$

be the time rate of change of the ensemble average of the line integral (5). Carrying out the ensemble averaging in the full Hamiltonian phase space, we have

$$\begin{aligned} \frac{d}{dt}\langle G \rangle &= \int_{\mathbb{R}^{2N}} d\mathbf{X} d\mathbf{P} g_i(\mathbf{x}) \frac{\partial H}{\partial P_i}(\mathbf{X}, \mathbf{P}) f(\mathbf{X}, \mathbf{P}, t) \\ &= \int_{\mathbb{R}^n} d\mathbf{x} g_i(\mathbf{x}) \left[\int_{\mathbb{R}^{N-n}} d\tilde{\mathbf{X}} \int_{\mathbb{R}^N} d\mathbf{P} \frac{\partial H}{\partial P_i} f(\mathbf{X}, \mathbf{P}, t) \right] \\ &= \int_{\mathbb{R}^n} d\mathbf{x} g_i(\mathbf{x}) J_i(\mathbf{x}, t), \end{aligned} \quad (14)$$

³More generally, it is less clear that one might infer this separation of timescales looking directly at the structure of the full H . Related to this point, there are certainly many Hamiltonian flows for which this form of separation of timescales is not expected [26].

where $J_i(\mathbf{x}, t)$ is the i th component of the projected probability current in (12). From (13) and (14), the previously mentioned line integral formula (6) follows.

We now examine two instructive special cases. If \mathbf{g} is the differential of a function $\phi(\mathbf{x})$, and so $\mathbf{g} = \nabla\phi$, we have

$$g_i J_i = \partial_i \phi J_i = \nabla\phi \cdot \mathbf{J}. \quad (15)$$

For stationary statistics, we have $\nabla \cdot \mathbf{J} = 0$, in which case we can write

$$g_i J_i = \nabla \cdot (\phi \mathbf{J}).$$

Hence, the integral (14) of $g_i J_i$ over a region of \mathbb{R}^N is a boundary integral. Assuming sufficiently strong decay of $\phi \mathbf{J}$ as $|\mathbf{x}| \rightarrow \infty$, the boundary integral vanishes as the region expands to the whole \mathbb{R}^N . Hence, $d\langle G \rangle/dt$ vanishes for stationary statistics. We conclude that a line integral of an exact differential form cannot detect irreversibility.

Next we look at the stochastic area [9,20] as a detector of irreversibility. Let

$$C(t): x_1 = x_1(t'), \quad x_2 = x_2(t'), \quad 0 < t' < t, \quad (16)$$

be the projection of a stochastic trajectory in the time interval $(0, t)$ onto the (x_1, x_2) plane. Then the line integral

$$A(t) := \frac{1}{2} \int_{C(t)} x_1 dx_2 - x_2 dx_1 \quad (17)$$

represents the area swept out by the displacement vector (x_1, x_2) in the time interval $0 < t' < t$. The net rotation of the displacement vector about the origin after a sufficiently long time indicates irreversibility. According to (14) and (17), the ensemble rate of change of area can be written in terms of J_i as

$$\frac{d}{dt}\langle A \rangle = \frac{1}{2} \int_{\mathbb{R}^n} d\mathbf{x} (x_1 J_2 - x_2 J_1). \quad (18)$$

IV. STOCHASTIC LINE INTEGRALS WITHIN REDUCED STATISTICS

Since the exact statistics of Hamiltonian phase-space trajectories projected onto the macroscopic state space is modeled by the SDE (1), it is natural to ask what the analog of the line integral formula (14) is within the reduced statistics. The analog of the right-hand side (RHS) of (14) seems clear enough: The exact probability current \mathbf{J} can be replaced by the Fokker-Planck probability current [cf. (7)]. A deeper question concerns how to implement line integrals over trajectories of the SDE (1). Here we examine two definitions of stochastic line integral closely, both of which are related to the Stratonovich stochastic integral [21].

The first proposed definition of stochastic line integral is

$$\int_{C(t)} g_i(\mathbf{x}) dx_i := \lim_{N \rightarrow \infty} \sum_{t'} g(\mathbf{y}(t')) dx_i(t'). \quad (19)$$

Here $t' := ndt$, $dt := t/N$, and the summation runs from $n = 0$ to $n = N$. The $dx_i(t')$ are components of the forward difference as in (2) and the $\mathbf{y}(t')$ are midpoints

$$\mathbf{y}(t') := \frac{\mathbf{x}(t') + \mathbf{x}(t' + dt)}{2}. \quad (20)$$

The evaluation of differential form components g_i at midpoints between $\mathbf{x}(t')$ and $\mathbf{x}(t' + dt)$ is analogous to the Stratonovich stochastic integral [21,25].

The second definition of the stochastic line integral replaces evaluation of the g_i at midpoints by the average at end points, that is,

$$\int_{C(t)} g_i(\mathbf{x}) dx_i := \lim_{N \rightarrow \infty} \sum_{t'} \frac{1}{2} [g_i(\mathbf{x}(t')) + g_i(\mathbf{x}(t' + dt))] dx_i(t'). \quad (21)$$

Here the summation is over $t' = ndt$, $0 \leq n < N$, as in the first definition (19). Let us look at the difference between the two definitions,

$$\lim_{N \rightarrow \infty} \sum_{t'} \left[\frac{1}{2} g_i(\mathbf{x}(t')) - g_i(\mathbf{y}(t')) + \frac{1}{2} g_i(\mathbf{x}(t' + dt)) \right] dx_i(t'). \quad (22)$$

Setting $\mathbf{x}(t') = \mathbf{y}(t') - \frac{1}{2} d\mathbf{x}(t')$ and $\mathbf{x}(t' + dt) = \mathbf{y}(t') + \frac{1}{2} d\mathbf{x}(t')$, we find that the Taylor polynomial approximation of the term in square brackets is quadratic in $d\mathbf{x}(t')$ and so is $O(dt)$. Then the entire sum in (22) is $O(Ndt^{3/2}) = O(\frac{1}{\sqrt{N}}) \rightarrow 0$ as $N \rightarrow \infty$. The limit process of the second definition yields the same result as the first. The reason for the second definition is that its equivalence to the first gives a reassuring sense that the notion of stochastic line integral is robust. In addition, the two definitions of stochastic line integral lead to two constructions of probability current based upon discrete time series of state variables, and close variants of both appear in the literature [9,14].

Our immediate task is to analyze the ensemble-averaged stochastic line integral according to the first definition (19). We take the time series $\mathbf{x}(t)$ to be a solution of the Itô SDE (1). Setting $\mathbf{y}(t') = \mathbf{x}(t') + \frac{1}{2} d\mathbf{x}(t')$ and evoking (2) for the forward difference $d\mathbf{x}(t')$, we have

$$\begin{aligned} & \langle g_i(\mathbf{y}(t')) dx_i(t') \rangle \\ &= \langle g_i(\mathbf{x}(t')) dx_i(t') \rangle + \frac{1}{2} \langle (\partial_j g_i) \mathbf{x}(t') dx_j(t') \rangle + O(dt^{3/2}) \\ &= \langle g_i(\mathbf{x}(t')) \sigma_{ij} dW_j(t') \rangle + \langle (g_i u_i) \mathbf{x}(t') \rangle dt \\ & \quad + \frac{1}{2} \langle (\partial_j g_i) \mathbf{x}(t') \sigma_{ik} \sigma_{jl} dW_k(t') dW_l(t') \rangle + O(dt^{3/2}). \end{aligned} \quad (23)$$

Since $\mathbf{x}(t')$ is independent of the increment $d\mathbf{W}(t')$ over the time interval $(t', t' + dt)$, we simplify the RHS to

$$\begin{aligned} & \langle g_i(\mathbf{x}(t')) \rangle \sigma_{ij} \langle dW_j(t') \rangle + \langle (g_i u_i) \mathbf{x}(t') \rangle \tau \\ & \quad + \frac{1}{2} \langle (\partial_j g_i) \mathbf{x}(t') \rangle \sigma_{ik} \sigma_{jl} \langle dW_k dW_l(t') \rangle + O(dt^{3/2}). \end{aligned} \quad (24)$$

Evoking the statistics of dW_i [cf. (3)], we can write

$$\langle g_i(\mathbf{y}(t')) dx_i(t') \rangle = \langle (g_i u_i + D_{ij} \partial_j g_i) \mathbf{x}(t') \rangle dt + O(dt^{3/2}). \quad (25)$$

Here D_{ij} are the components of the diffusion tensor in (8). Hence,

$$\begin{aligned} & \left\langle \sum g_i(\mathbf{y}(t')) dx_i(t') \right\rangle \\ &= \sum \langle (g_i u_i + D_{ij} \partial_j g_i) \mathbf{x}(t') \rangle dt + O\left(\frac{1}{\sqrt{N}}\right). \end{aligned} \quad (26)$$

The RHS is the Riemann sum for the integral of $\langle (g_i u_i + D_{ij} \partial_j g_i) \mathbf{x}(t') \rangle$ over $0 < t' < t$, so we have

$$\left\langle \int_{C(t)} g_i(\mathbf{x}) dx_i \right\rangle = \int_0^t dt' \langle (g_i u_i + D_{ij} \partial_j g_i) \mathbf{x}(t') \rangle. \quad (27)$$

Introducing the reduced probability density $\rho(\mathbf{x}, t)$, we have

$$\begin{aligned} \langle g_i u_i + D_{ij} \partial_j g_i \rangle &= \int_{\mathbb{R}^n} d\mathbf{x} \rho (g_i u_i + D_{ij} \partial_j g_i) \\ &= \int_{\mathbb{R}^n} d\mathbf{x} g_i (\rho u_i - D_{ij} \partial_j \rho). \end{aligned} \quad (28)$$

Here we recognize the components of the Fokker-Planck probability current (7) or, equivalently, the reduced probability current density. Thus, Eqs. (27) and (28) allow us to write the line integral formula within the reduced statistics,

$$\frac{d}{dt} \langle G \rangle = \int_{\mathbb{R}^n} d\mathbf{x} g_i j_i. \quad (29)$$

This equation has the same form as (14) with projected probability current \mathbf{J} now replaced by the Fokker-Planck current \mathbf{j} and reaffirms the role of the stochastic line integrals as a detector of irreversibility. For steady-state situations (i.e., $\partial \mathbf{j} / \partial t = 0$), if we have $\mathbf{j} = 0$ everywhere in the reduced phase space, then $d\langle G \rangle / dt$ vanishes for any choice of vector function \mathbf{g} and detailed balance is satisfied. Conversely, if \mathbf{j} has regions of nonzero value, one can choose \mathbf{g} such that $d\langle G \rangle / dt \neq 0$ with the magnitude and sign determined according to (29), thereby providing a quantitative measure of the associated irreversible behavior. Suitable choices of \mathbf{g} will typically depend on system details; examples are discussed in the following section.

V. IRREVERSIBLE STATISTICS OF COUPLED BROWNIAN PARTICLES: STREAM-FUNCTION APPROACH

We analyze the overdamped statistics of two degrees of freedom with coordinates x_1 and x_2 in a given energy landscape $U(x_1, x_2)$. The following are two major reasons for studying this type of system: (i) The physics is analogous to that of many physical nonequilibrium systems that are the focus of recent work including coupled electronic circuits and mechanical systems [2,9,23,30] and (ii) the reduction of high-dimensional systems onto two-dimensional planar subspaces often has a similar effective dynamics [1,11]. The Itô SDE system for $x_1(t)$ and $x_2(t)$ can be written as

$$dx_1 = -\mu_1 \partial_1 U dt + \sigma_1 dW_1, \quad dx_2 = -\mu_2 \partial_2 U dt + \sigma_2 dW_2, \quad (30)$$

where μ_1 and μ_2 are given mobilities, dW_1 and dW_2 are forward differences of independent Wiener processes, and σ_1 and σ_2 are given noise amplitudes. Following previous studies [12,14,30], we can think of (30) as the stochastic dynamics of two Brownian particles in heat baths of temperatures T_1 and T_2 . Each particle moves in its own potential, which may be nonlinear, and we assume below that they are coupled to one another with a linear (or nonlinear) spring (cf. Fig. 1). The noise amplitudes are related to the temperatures by the usual Einstein relations [25]

$$\sigma_1 = \sqrt{2\mu_1 k_B T_1}, \quad \sigma_2 = \sqrt{2\mu_2 k_B T_2}. \quad (31)$$

We now focus on the specific form taken by the line integral formula (29) for stationary statistics of the two-dimensional stochastic dynamics of (30). The stationary probability current \mathbf{j} on \mathbb{R}^2 is divergence free, so there exists a stream function $\psi(\mathbf{x})$ satisfying [31]

$$j_1 = \partial_2 \psi, \quad j_2 = -\partial_1 \psi. \quad (32)$$

Assuming that \mathbf{j} decays to zero sufficiently rapidly as $|\mathbf{x}| \rightarrow \infty$, we may select the unique stream function which vanishes at infinity. The reason for this selection becomes evident momentarily: Substituting (32) for j_1 and j_2 into the line integral formula (29), we have

$$\frac{d}{dt} \langle G \rangle := \int_{\mathbb{R}^2} d\mathbf{x} (g_1 \partial_2 \psi - g_2 \partial_1 \psi) = \int_{\mathbb{R}^2} d\mathbf{x} \psi (\partial_1 g_2 - \partial_2 g_1), \quad (33)$$

where the second equality uses integration by parts and the boundary condition that ψ vanishes at ∞ . For stochastic area (18) ($g_1 = -\frac{x_2}{2}$ and $g_2 = \frac{x_1}{2}$), the ensemble-averaged rate of change can be written concisely in terms of the stream function

$$\frac{d}{dt} \langle A \rangle = \int_{\mathbb{R}^2} d\mathbf{x} \psi. \quad (34)$$

This remarkable formula shows a simple and direct connection between the stochastic area and the stream function. For some problems it may be relatively easy to compute or even calculate ψ and (34) provides a direct connection to ensemble-averaged time rate of change of area, thus providing a quantitative measure of system irreversibility [9,14].

We now formulate a boundary value problem for the stream function, noting that equations of this type have been studied extensively in hydrodynamics, with a large arsenal of solution methods available [31,32]. Recalling that $j_i = -\mu_i \partial_i U \rho - \frac{1}{2} \sigma_i^2 \partial_i \rho$, we can recast the stream-function derivatives in (32) as

$$\partial_2 \psi = -\mu_1 \rho \partial_1 U - \frac{1}{2} \sigma_1^2 \partial_1 \rho, \quad \partial_1 \psi = \mu_2 \rho \partial_2 U + \frac{1}{2} \sigma_2^2 \partial_2 \rho. \quad (35)$$

Now we use these expressions to evaluate the combination $-\sigma_1^2 \partial_1 (\partial_1 \psi / \rho) - \sigma_2^2 \partial_2 (\partial_2 \psi / \rho)$ to arrive at

$$-\sigma_1^2 \partial_1 \left(\frac{\partial_1 \psi}{\rho} \right) - \sigma_2^2 \partial_2 \left(\frac{\partial_2 \psi}{\rho} \right) = (\sigma_2^2 \mu_1 - \sigma_1^2 \mu_2) \partial_{12} U. \quad (36)$$

With the help of (31), the prefactor $\sigma_2^2 \mu_2 - \sigma_1^2 \mu_1$ on the RHS of (36) is $2\mu_1 \mu_2 (T_2 - T_1)$, so the stream function $\psi(\mathbf{x})$ satisfies

$$-\sigma_1^2 \partial_1 \left(\frac{\partial_1 \psi}{\rho} \right) - \sigma_2^2 \partial_2 \left(\frac{\partial_2 \psi}{\rho} \right) = 2\mu_1 \mu_2 (T_2 - T_1) \partial_{12} U, \quad (37)$$

an inhomogeneous elliptical partial differential equation. The operator

$$-\sigma_1^2 \partial_1 \left(\frac{\partial_1}{\rho} \right) - \sigma_2^2 \partial_2 \left(\frac{\partial_2}{\rho} \right) \quad (38)$$

on the LHS is positive, i.e.,

$$\begin{aligned} & \int_{\mathbb{R}^2} d\mathbf{x} \varphi \left\{ -\sigma_1^2 \partial_1 \left(\frac{\partial_1 \varphi}{\rho} \right) - \sigma_2^2 \partial_2 \left(\frac{\partial_2 \varphi}{\rho} \right) \right\} \\ &= \int_{\mathbb{R}^2} d\mathbf{x} \left\{ \sigma_1^2 \frac{(\partial_1 \varphi)^2}{\rho} + \sigma_2^2 \frac{(\partial_2 \varphi)^2}{\rho} \right\} > 0, \end{aligned} \quad (39)$$

for all reasonably behaved $\varphi(\mathbf{x})$ that satisfy zero boundary conditions and are not identically constant. Hence, the solution to (37) subject to ψ vanishing at infinity is unique. It should be noted that the preceding analysis assumes a diagonal diffusion tensor [cf. (8)]. We also note that a more general boundary value problem and corresponding uniqueness theorem for the stream function can be established for the case of a general diffusion tensor and is treated elsewhere [33].

If the degrees of freedom are uncoupled ($\partial_{12} U = 0$) or the temperatures are equal ($T_1 = T_2$), then the stream function, and hence probability current, vanishes identically [cf. (37)]. Equivalently, the time rate of change of ensemble-averaged line integrals vanishes [cf. (34)].

We now examine the prototypical example of linearly coupled degrees of freedom with energy landscape

$$U(x_1, x_2) = u_1(x_1) + u_2(x_2) + \frac{k}{2}(x_2 - x_1)^2. \quad (40)$$

Here we treat $u_1(x_1)$ and $u_2(x_2)$ as potential energies of restoring forces acting on each degree of freedom separately. The two degrees of freedom are coupled by a spring with stiffness $k > 0$. We assume that $u_1(x)$ and $u_2(x)$ diverge to $+\infty$ as $|x| \rightarrow \infty$ sufficiently rapidly so that there is stationary probability density satisfying the usual normalization condition $\int_{\mathbb{R}^2} \rho d\mathbf{x} = 1$. For the energy (40), we have $\partial_{12} U = -k < 0$, and then the RHS of (37) is a positive constant for $T_1 > T_2$. Due to the positivity of the operator (38) and utilizing the maximum principle for elliptic partial differential equations [34], we conclude that $\psi > 0$ for $T_1 > T_2$. Then the rate of change of stochastic area in (34) is positive. This is consistent with the circulation of probability current: The stream function has a global maximum and the circulation of probability current sufficiently close to this maximum is counterclockwise. A similar argument for the case $T_1 < T_2$ results in $d\langle A \rangle / dt < 0$ and clockwise circulation near the global minimum of ψ .

Next we show that the rate of heat transfer between baths is the rate of change of a similar stochastic line integral. To see this, note that the forward difference of the energy (40) is

$$\begin{aligned} dU &= \partial_1 U dx_1 + \partial_2 U dx_2 + \frac{1}{2} \partial_{11} U (dx_1)^2 \\ &+ \partial_{12} U dx_1 dx_2 + \partial_{22} U (dx_2)^2 + O(dt^{3/2}). \end{aligned} \quad (41)$$

Substituting for dx_1 and dx_2 according to the Itô SDE (30) and using the identities (3) satisfied by dW_1 and dW_2 , the ensemble average of (41) yields

$$\frac{d}{dt} \langle U \rangle = -\dot{Q}_1 - \dot{Q}_2, \quad (42)$$

where

$$\dot{Q}_1 := \mu_1 \langle (\partial_1 U)^2 \rangle - \frac{\sigma_1^2}{2} \langle \partial_{11} U \rangle, \quad (43)$$

$$\dot{Q}_2 := \mu_2 \langle (\partial_2 U)^2 \rangle - \frac{\sigma_2^2}{2} \langle \partial_{22} U \rangle. \quad (44)$$

For stationary statistics, $\langle U \rangle$ is time independent, so \dot{Q}_1 and $-\dot{Q}_2$ have a common value, which we denote by \dot{Q} . In the formula (43) for \dot{Q}_1 , we interpret $\mu_1 \langle (\partial_1 U)^2 \rangle$ as the rate of heating of bath 1 by dissipation and $\frac{1}{2} \sigma_1^2 \langle \partial_{11} U \rangle$ as the rate at which bath 1 induced noisy fluctuations impart energy to the mass. Hence, \dot{Q} is the net rate of energy transfer into bath 1 and we can express \dot{Q} as the rate of change of the ensemble average of the stochastic line integral

$$q(t) := -\frac{1}{2} \int_{C(t)} \partial_1 U dx_1 - \partial_2 U dx_2. \quad (45)$$

Carrying out the ensemble and using (29) with $g_1 = -\frac{1}{2} \partial_1 U$ and $g_2 = \frac{1}{2} \partial_2 U$, we have

$$\frac{d}{dt} \langle q \rangle = -\frac{1}{2} \int_{\mathbb{R}^2} (\partial_1 U j_1 - \partial_2 U j_2) d\mathbf{x}. \quad (46)$$

Substituting

$$j_1 = -\mu_1 \partial_1 U \rho - \frac{\sigma_1^2}{2} \partial_1 \rho, \quad j_2 = -\mu_2 \partial_2 U \rho - \frac{\sigma_2^2}{2} \partial_2 \rho,$$

we readily find

$$\frac{d}{dt} \langle q \rangle = \frac{1}{2} (\dot{Q}_1 - \dot{Q}_2) = \dot{Q}. \quad (47)$$

Alternatively, we substitute $j_1 = \partial_2 \psi$ and $j_2 = -\partial_1 \psi$ into (46) to find

$$\dot{Q} = \frac{d}{dt} \langle q \rangle = \int_{\mathbb{R}^2} d\mathbf{x} \psi \partial_{12} U, \quad (48)$$

and we see that there is *no* heat transfer if the degrees of freedom are uncoupled or the temperatures of the baths are equal. For linear coupling with $\partial_{12} U := -k < 0$, Eq. (48) reduces to

$$\dot{Q} = -k \frac{d}{dt} \langle A \rangle, \quad (49)$$

where $d\langle A \rangle/dt$ is the rate of change of ensemble-averaged stochastic area. For $T_1 > T_2$ we have $d\langle A \rangle/dt > 0$ and $\dot{Q} < 0$, and for $T_1 < T_2$, $\dot{Q} < 0$, as expected. It is interesting to note that the expression (48) also applies to the case of nonlinear coupling spring. For a variety of different nonlinear couplings (e.g., cubic, quartic, and Lennard-Jones) there will be a corresponding set of stochastic line integrals that utilize distinct vector \mathbf{g} functions.

In principle, $d\langle A \rangle/dt$, and hence \dot{Q} , is a function of the noise amplitudes σ_1 and σ_2 or, equivalently, the bath temperatures T_1 and T_2 . We first consider linear stochastic dynamics, with

$$u_1(x) = u_2(x) = \frac{K}{2} x^2. \quad (50)$$

From the theory of linear stochastic dynamics worked out in [20], we readily find

$$\frac{d}{dt} \langle A \rangle = \frac{k^2}{k + K} \frac{\mu_2 \sigma_1^2 - \mu_1 \sigma_2^2}{\mu_1 + \mu_2}. \quad (51)$$

Using (31), we can then express $d\langle A \rangle/dt$ in terms of temperatures as

$$\frac{d}{dt} \langle A \rangle = \frac{\mu_1 \mu_2}{\mu_1 + \mu_2} \frac{k}{K + k} k_B (T_1 - T_2). \quad (52)$$

Now we use (49) to write the heat transfer rate as

$$\dot{Q} = \frac{\mu_1 \mu_2}{\mu_1 + \mu_2} \frac{k^2}{K + k} k_B (T_1 - T_2), \quad (53)$$

and it can be seen that the rate of heat transfer from bath 1 to bath 2 is simply proportional to the temperature difference $T_2 - T_1$.

We test (52) by direct numerical solution of the SDE for the spring-coupled masses (30). For numerical work, we use dimensionless units and we take $\mu_1 = \mu_2 = \mu$ (common value). We assume x_1 and x_2 are dimensionless and we let E denote a characteristic energy associated with $U(x_1, x_2)$. The unit of time is $(\mu E)^{-1}$ and noise amplitudes are measured in units of $\sqrt{\mu E}$. Working with dimensionless units, we set $\mu_1 = \mu_2 = 1$ in the SDE (30). Then the dimensionless energy [cf. (40)] for linear stochastic dynamics is

$$U(x_1, x_2) = \frac{1}{2} x_1^2 + \frac{1}{2} x_2^2 + \frac{\epsilon}{2} (x_2 - x_1)^2, \quad (54)$$

where $\epsilon := \frac{k}{K}$. We can also write (52) for $d\langle A \rangle/dt$ in dimensionless form as

$$\frac{d}{dt} \langle A \rangle = \frac{1}{2} \frac{\epsilon^2}{1 + \epsilon} (\sigma_1^2 - \sigma_2^2). \quad (55)$$

Now let $x_1[t]$ and $x_2[t]$ be discrete time series of x_1 and x_2 obtained by standard Euler-Maruyama iterations with time step τ , starting from zero initial conditions. The discrete Stratonovich approximation to the stochastic area at time $t = N\tau$, N a positive integer, is

$$A(t) = \sum_{n=0}^{N-1} dA(n\tau), \quad (56)$$

where

$$dA(t) := \frac{1}{2\tau} [x_1(t)x_2(t + \tau) - x_1(t + \tau)x_2(t)]. \quad (57)$$

Figure 3 presents numerical results for $A(t)/t$ for two independent trials associated with distinct realizations of the noisy term but with common statistics. The parameter values are $\epsilon = 1.0$, $\sigma_1 = 2.0$, and $\sigma_2 = 1.0$. We perform two independent runs, the first of which has 10^6 time steps with step size $\tau = 0.01$. The second, with twice as many time steps and half the step size, provides a straightforward confirmation of numerical convergence. Given a numerical time series of $A(t)$, we plot $A(t)/t$ versus elapsed time t (logarithmic scale). The (blue) circles are obtained from the first run with 10^6 time steps. In the limit of large times, we observe convergence to a constant value $A(t)/t \approx 0.747$ for $t \gg 1$. The (red) squares are obtained from the second run with 2×10^6 time steps. The initial transient is different, since noise forcings for different simulations are independent. The second run gives $A(t)/t \approx 0.750$ for $t \gg 1$, consistent with the value from the first run. Furthermore, both values are consistent with the theoretical prediction based on (55), which evaluates to $d\langle A \rangle/dt = 3/4$ for the indicated parameters.

Figure 4 displays the dependence of $d\langle A \rangle/dt$ upon the noise amplitude $\sigma := \sigma_1$ with fixed ratio $r := \sigma_2/\sigma_1 = 0.5$. Numerical calculations are carried out for a sequence of σ_1 values in the range 0–2.0. The circles represent estimates of

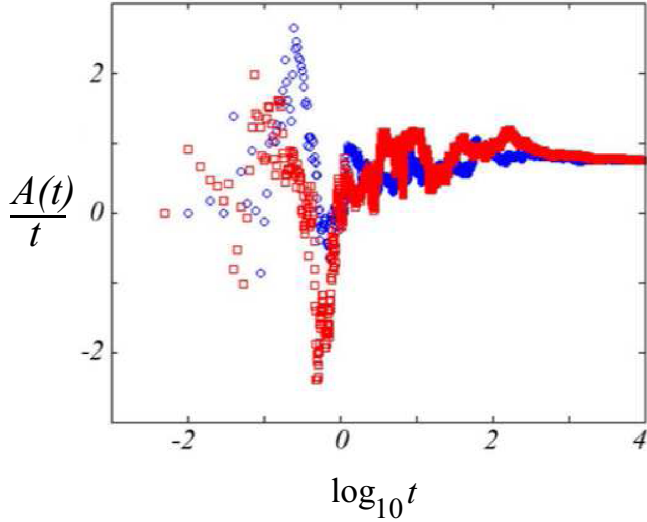


FIG. 3. Plot of $A(t)/t$ vs t computed for two independent stochastic trials for the two-dimensional system described by (30) with potential energy given by (54) and with parameter values $\epsilon = 1.0$, $\sigma_1 = 2.0$, and $\sigma_2 = 1.0$. For large t , both trials converge to a common value corresponding to the stationary state.

$d\langle A \rangle/dt$ based upon computed values of $A(t)/t$ for elapsed time $t = 10^4$. The solid curve represents the theoretical dependence of $d\langle A \rangle/dt$ upon σ_1 with $\sigma_2/\sigma_1 = 0.5$ evaluated according to (55). Numerical data are clearly consistent with quadratic scaling that is predicted by (55). In contrast, the square data points associated with the lower curve are obtained with a nonlinear restoring force and discussed in the following section.

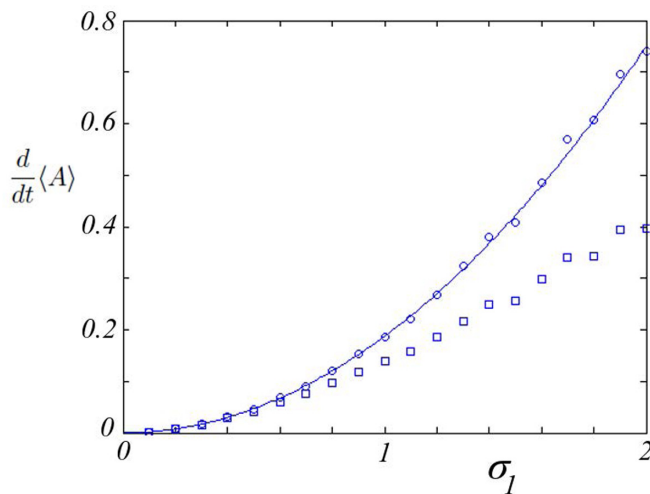


FIG. 4. Dependence of time rate of change of stochastic area as a function of noise amplitude σ_1 for linear (circles) and nonlinear (squares) restoring forces; cf. potential energy expressions (54) and (58), respectively. The ratio $\sigma_2/\sigma_1 = 0.5$ is fixed. In the linear case, the solid theoretical curve is obtained by direct evaluation of (55).

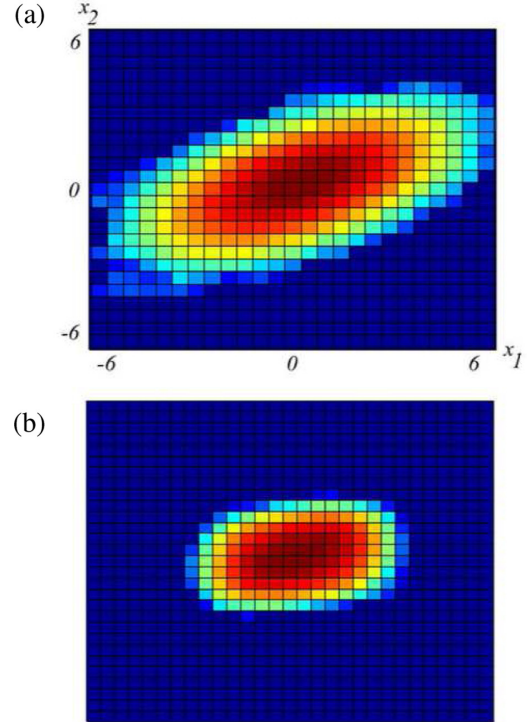


FIG. 5. Stationary probability density histograms for systems driven by identical noise amplitudes: (a) linear restoring force derived from (54) and (b) nonlinear restoring force derived from (58), both with parameter choice $\epsilon = 1$.

VI. EFFECTS OF NONLINEARITY: SCALING OF STOCHASTIC AREA WITH NOISE INTENSITY

The dependence of $d\langle A \rangle/dt$ upon noise amplitudes is modified by nonlinearity. Related to this, the square data points in Fig. 4 represent numerical values of $d\langle A \rangle/dt$ obtained by using a potential energy function

$$U(x_1, x_2) = u(x_1) + u(x_2) + \frac{\epsilon}{2}(x_2 - x_1)^2, \quad (58)$$

with $u(x)$ given by

$$u(x) = \frac{1}{2}x^2 + \frac{1}{4}x^4. \quad (59)$$

This corresponds to a stiff spring; at small vibrational amplitude the restoring force is linear, while at larger amplitudes the positive quartic term is associated with a increasing effective spring constant. As σ increases from 0 to 2.0, the dependence of $d\langle A \rangle/dt$ upon σ transitions from quadratic to approximately linear, a trend that can be understood qualitatively as follows. For increasing noise amplitude, characteristic deviations from the mechanical equilibrium $x_1 = x_2 = 0$ also increase. Trajectories induced by sufficiently strong noise preferentially sample the nonlinear part of the restoring force which is more confining than the linear part, and thus the stochastic area growth rate is inhibited relative to a purely linear restoring force. The nonlinearity-enhanced confinement is also evident by comparing probability density histograms of linear and nonlinear cases driven by identical noise amplitudes (cf. Fig. 5).

We now turn to analyzing the dependence of stochastic area upon noise amplitudes using the stream function. In particular, we want to quantitatively understand the aforementioned confinement effect, whereby hard spring nonlinearity reduces the increase of heat transfer as the noise temperatures increase. We work in the dimensionless formulation with $\mu_1 = \mu_2 = 1$ with dimensionless energy landscape given by (58) and (59). In order to implement a scaling argument we focus here on the case of weak coupling $0 < \epsilon \ll 1$ and $u(x)$ homogeneous of degree $n > 0$ so that

$$u(ax) = a^n u(x) \tag{60}$$

for all x and $a > 0$. We take the noise amplitudes to be

$$\sigma_1 = \sigma, \quad \sigma_2 = \sigma r, \tag{61}$$

where σ is any positive constant and r denotes the ratio of noise amplitudes σ_2/σ_1 [35]. For $\epsilon = 0$, the stationary probability density is proportional to the product of the effective Boltzmann factors of the two decoupled degrees of freedom,

$$\rho \sim \rho_0 \propto \exp\left(-\frac{u(x_1)}{\sigma_1^2}\right) \exp\left(-\frac{u(x_2)}{\sigma_2^2}\right). \tag{62}$$

The leading $\epsilon \rightarrow 0$ approximation to the stream function $\psi(\mathbf{x})$ then satisfies

$$-\partial_1 \left(\frac{1}{\rho_0} \partial_1 \psi \right) - r^2 \partial_2 \left(\frac{1}{\rho_0} \partial_2 \psi \right) = \epsilon(1 - r^2). \tag{63}$$

This equation is obtained by setting $\mu_1 = \mu_2 = 1$ in (36), substituting (61) for σ_1 and σ_2 , replacing ρ by ρ_0 , and setting $\partial_{12}U = -\epsilon$ as follows from (58). Notice the cancellation of the factor σ^2 from both sides.

In analogy with certain boundary layer problems in two-dimensional fluid systems, we note that the solutions of (63) possess a scaling symmetry [32]. Thus, letting $R(\mathbf{x})$ denote the probability density (62) for $\sigma = 1$, we can express the probability density for any $\sigma > 0$ as

$$\rho_0(\mathbf{x}) = \frac{1}{\sigma^{4/n}} R\left(\boldsymbol{\xi} := \frac{\mathbf{x}}{\sigma^{2/n}}\right). \tag{64}$$

Now let $\Psi(\boldsymbol{\xi})$ denote the stream function for $\sigma = 1$. We seek the stream function for any $\sigma > 0$ as

$$\psi(\mathbf{x}) = b\Psi(\boldsymbol{\xi}), \tag{65}$$

where the constant b is to be determined. Substituting this form into (63), we have

$$-b \left[\frac{\partial}{\partial \xi_1} \left(\frac{1}{R} \frac{\partial \Psi}{\partial \xi_1} \right) + \sigma^2 \frac{\partial}{\partial \xi_2} \left(\frac{1}{R} \frac{\partial \Psi}{\partial \xi_2} \right) \right] = \epsilon(1 - r^2), \tag{66}$$

which has the exact form of the original equation (63) for ψ when $\sigma = 1$ provided we choose $b = 1$. Hence, we conclude that

$$\psi(\mathbf{x}) = \Psi\left(\frac{\mathbf{x}}{\sigma^{2/n}}\right). \tag{67}$$

Using this result, we can now write the rate of change of stochastic area (34) as

$$\frac{d}{dt} \langle A \rangle = \int_{\mathbb{R}^2} \Psi\left(\frac{\mathbf{x}}{\sigma^{2/n}}\right) d\mathbf{x} = \sigma^{4/n} \int_{\mathbb{R}^2} \Psi(\boldsymbol{\xi}) d\boldsymbol{\xi} \tag{68}$$

and hence $d\langle A \rangle/dt$ scales as

$$\frac{d}{dt} \langle A \rangle \propto \sigma^{4/n}. \tag{69}$$

For linear stochastic dynamics associated with a quadratic potential energy function ($n = 2$), we have $d\langle A \rangle/dt \propto \sigma^2$, a quadratic dependence on noise amplitude. However, for the case of quartic confining potential with $n = 4$, we find $d\langle A \rangle/dt \propto \sigma$, so area growth grows only linearly with noise amplitude. Recall that the numerical graph of $d\langle A \rangle/dt$ versus σ_1 with $\sigma_2/\sigma_1 = 0.50$ in Fig. 4 is apparently linear for $\sigma_1 > 1$. Since temperatures T_1 and T_2 are proportional to $\sigma_1^2 = \sigma^2$ and $\sigma_2^2 = \sigma^2 r^2$, we rewrite (69) as

$$\frac{d}{dt} \langle A \rangle \propto (\sigma^2)^{2/n}. \tag{70}$$

For linear stochastic dynamics with $n = 2$, we see that $d\langle A \rangle/dt$ increases linearly with increasing temperatures, consistent with (45). For stiff nonlinearity with $n > 2$, the increase of $d\langle A \rangle/dt$ with temperatures is sublinear.

VII. CONCLUDING DISCUSSION

A general framework has been presented for understanding the use of stochastic line integrals to quantitatively characterize dynamical behavior in noise-driven nonequilibrium systems. The concept of SLI has been shown to apply both at the level of high-dimensional phase space associated with Hamiltonian flow that includes all the microscopic degrees of freedom and in the reduced phase space typically described by a SDE. The implementation has been shown to be robust and numerical implementation schemes have been described. We have also shown how general results play out in detail for a paradigmatic model system: two coupled mass-spring elements at different temperatures. Along the way, SLIs were developed that correspond to physically meaningful quantities such as heat flow. We have shown that the stochastic line integral of any nonexact differential form vanishes in a detailed balance system, so its nonvanishing is a clear imprimatur of irreversibility. In summary, stochastic line integrals are robust indicators of irreversibility which can be calculated directly from experimental time series. Collateral deductions of heat transfer (if appropriate) readily follow. For many experimental systems (e.g., biophysical systems) this route may be more accessible than carrying out calorimetry. A recent example of determination of stochastic area directly from experimental data is found in [9], which examines the dynamics of two coupled electronic circuits driven by nonequilibrium noise sources. More generally, determination of an SLI from experimental data requires access to the time series of the coordinates that define the particular SLI. We note that, in addition to noise-driven electronic circuit systems, the appropriate type of data is also available for biological systems using time-dependent microscopy [1,2].

We have also shown how the average growth rate of stochastic line integrals on two-dimensional state spaces can be evaluated with the aid of stream functions. However, there are certainly straightforward approaches that do not require use of stream functions. For example, one can solve the Fokker-Planck equation, extract the collateral probability

current, and then determine the average growth of the desired stochastic line integral by explicit evaluation of (29). What then are the relative advantages to using a stream-function approach? Among them, we have shown how the stream-function formulation clearly connects to essential physical properties such as area growth rate and heat transport. In the elliptic equation (37) for ψ , the source term on the RHS contains the product $(T_1 - T_2)\partial_{12}U$, so one can see directly why the temperature difference and actual coupling ($\partial_{12}U$ not identically zero) are both essential for irreversibility. Another benefit of the stream-function formulation is that scaling arguments like the one presented in Sec. VI are vastly more accessible.

Strictly speaking, the stream-function analysis of probability current is limited to systems with two degrees of freedom. However, in practice, experimentalists often probe high-dimensional statistics by various two-dimensional projections [1]. For any such projection, there *is* a stream function for the probability current in the plane of the projection. To see this, note that the probability density $f(\mathbf{x})$ for $\mathbf{x} \in \mathbb{R}^n$ with $n > 2$ satisfies the continuity equation

$$\partial_t f + \partial_1 j_1 + \cdots + \partial_n j_n = 0. \quad (71)$$

Here j_1, \dots, j_n are components of the probability current in \mathbb{R}^n . The marginal with respect to two variables, say, x_1 and x_2 , is

$$\rho(x_1, x_2, t) := \int_{\mathbb{R}^{n-2}} f(\mathbf{x}) dx_3 \cdots dx_n. \quad (72)$$

It satisfies the two-dimensional continuity equation

$$\partial_t \rho + \partial_1 J_1 + \partial_2 J_2 = 0, \quad (73)$$

where

$$J_1(x_1, x_2, t) := \int_{\mathbb{R}^{n-2}} j_1(\mathbf{x}) dx_3 \cdots dx_n \quad (74)$$

and similarly for $J_2(x_1, x_2, t)$. The projected current

$$\mathbf{J} = \begin{pmatrix} J_1 \\ J_2 \end{pmatrix} \quad (75)$$

in the (x_1, x_2) plane is generally not expressible as a drift-diffusion functional determined only by the marginal density ρ . Nevertheless, certain general conclusions apply. For stationary statistics with $\partial_t \rho = 0$, the projected current (75) is divergence-free, so it has a stream function $\psi(x_1, x_2)$. The integral curves of the projected current are level curves of this stream function. Assuming the usual boundary condition $\psi \rightarrow 0$ as $|x_1|$ or $|x_2| \rightarrow \infty$, we typically have closed, nested level curves of ψ . We also note that the expressions for various SLIs in terms of stream functions, e.g., (33) and (34), remain valid when one uses stream functions determined using the aforementioned projection procedure. Additionally, we note that, provided an experiment can measure time series for at least two independent variables, the determination of SLIs such as stochastic area is possible. If one has access to more than two variables in a higher-dimensional system, one can measure SLIs corresponding to all possible pairwise combinations or, equivalently, different two-dimensional projections. Then the observation of a nonzero time rate of change in any one of the SLIs thus constructed implies that the higher-dimensional system is irreversible.

Finally, we point to one conspicuous direction for future work: the case of state-dependent noise. There are physical contexts in which it appears unavoidable, such as circuits containing elements with nonlinear current-voltage relations [10]. Presumably, one still has recorded time series of state variables and its natural to ask whether (suitably modified) stochastic line integrals of nonexact differential forms allow us to read irreversibility and calculate heat transfer and entropy production in such situations.

ACKNOWLEDGMENT

We thank Konstantin Matveev for helpful discussions.

-
- [1] C. Battle, C. P. Broedersz, N. Fakhri, V. F. Geyer, J. Howard, C. F. Schmidt, and F. C. MacKintosh, Broken detailed balance at mesoscopic scales in active biological systems, *Science* **352**, 604 (2016).
 - [2] F. Gnesotto, F. Mura, J. Gladrow, and C. P. Broedersz, Broken detailed balance and non-equilibrium dynamics in living systems: A review, *Rep. Prog. Phys.* **81**, 066601 (2018).
 - [3] J. B. Weiss, Fluctuation properties of steady-state Langevin systems, *Phys. Rev. E* **76**, 061128 (2007).
 - [4] J. B. Weiss, B. Fox-Kemper, D. Mandal, A. D. Nelson, and R. K. P. Zia, Nonequilibrium Oscillations, Probability Angular Momentum, and the Climate System, *J. Stat. Phys.* **179**, 1010 (2020).
 - [5] J. Gieseler, R. Quidant, C. Dellago, and L. Novotny, Dynamic relaxation of a levitated nanoparticle from a non-equilibrium steady state, *Nat. Nanotechnol.* **9**, 358 (2014).
 - [6] J. Millen, T. Deesuan, P. Barker, and J. Anders, Nanoscale temperature measurements using non-equilibrium Brownian dynamics of a levitated nanosphere, *Nat. Nanotechnol.* **9**, 425 (2014).
 - [7] C. Gonzalez-Ballester, M. Aspelmeyer, L. Novotny, R. Quidant, and O. Romero-Isart, Levitodynamics: Levitation and control of microscopic objects in vacuum, *Science* **374**, eabg3027 (2021).
 - [8] Y. Bomze, R. Hey, H. T. Grahn, and S. W. Teitsworth, Noise-Induced Current Switching in Semiconductor Superlattices: Observation of Nonexponential Kinetics in a High-Dimensional System, *Phys. Rev. Lett.* **109**, 026801 (2012).
 - [9] J. P. Gonzalez, J. C. Neu, and S. W. Teitsworth, Experimental metrics for detection of detailed balance violation, *Phys. Rev. E* **99**, 022143 (2019).
 - [10] S. W. Teitsworth, M. E. Olson, and Y. Bomze, Scaling properties of noise-induced switching in a bistable tunnel diode circuit, *Eur. Phys. J. B* **92**, 74 (2019).

- [11] S. Ciliberto, A. Imparato, A. Naert, and M. Tanase, Heat Flux and Entropy Produced by Thermal Fluctuations, *Phys. Rev. Lett.* **110**, 180601 (2013).
- [12] S. Ciliberto, A. Imparato, A. Naert, and M. Tanase, Statistical properties of the energy exchanged between two heat baths coupled by thermal fluctuations, *J. Stat. Mech.* (2013) P12014.
- [13] H. C. Fogedby and A. Imparato, Heat flow in chains driven by thermal noise, *J. Stat. Mech.* (2012) P04005.
- [14] J. Li, J. M. Horowitz, T. R. Gingrich, and N. Fakhri, Quantifying dissipation using fluctuating currents, *Nat. Commun.* **10**, 1666 (2019).
- [15] R. K. P. Zia and B. Schmittmann, Probability currents as principal characteristics in the statistical mechanics of non-equilibrium steady states, *J. Stat. Mech.* (2007) P07012.
- [16] A. Mellor, M. Mobilia, and R. K. P. Zia, Characterization of the nonequilibrium steady state of a heterogeneous nonlinear q-voter model with zealotry, *Europhys. Lett.* **113**, 48001 (2016).
- [17] G. Gradziuk, F. Mura, and C. P. Broedersz, Scaling behavior of nonequilibrium measures in internally driven elastic assemblies, *Phys. Rev. E* **99**, 052406 (2019).
- [18] F. S. Gnesotto, G. Gradziuk, P. Ronceray, and C. P. Broedersz, Learning the non-equilibrium dynamics of Brownian movies, *Nat. Commun.* **11**, 5378 (2020).
- [19] A. Frishman and P. Ronceray, Learning Force Fields from Stochastic Trajectories, *Phys. Rev. X* **10**, 021009 (2020).
- [20] A. Ghanta, J. C. Neu, and S. Teitworth, Fluctuation loops in noise-driven linear dynamical systems, *Phys. Rev. E* **95**, 032128 (2017).
- [21] C. Gardiner, *Stochastic Methods: A Handbook for the Natural and Social Sciences*, *Springer Series in Synergetics* (Springer, Berlin, 2009).
- [22] L. Onsager, Reciprocal relations in irreversible processes. I. *Phys. Rev.* **37**, 405 (1931).
- [23] K.-H. Chiang, C.-L. Lee, P.-Y. Lai, and Y.-F. Chen, Entropy production and irreversibility of dissipative trajectories in electric circuits, *Phys. Rev. E* **95**, 012158 (2017).
- [24] J. Gladrow, N. Fakhri, F. C. MacKintosh, C. F. Schmidt, and C. P. Broedersz, Broken Detailed Balance of Filament Dynamics in Active Networks, *Phys. Rev. Lett.* **116**, 248301 (2016).
- [25] N. G. Van Kampen, *Stochastic Processes in Physics and Chemistry*, 3rd ed. (Elsevier, Amsterdam, 2007).
- [26] R. Zwanzig, *Nonequilibrium Statistical Mechanics* (Oxford University Press, Oxford, 2001).
- [27] C. H. Bennett, The thermodynamics of computation—A review, *Int. J. Theor. Phys.* **21**, 905 (1982).
- [28] R. C. Tolman, *The Principles of Statistical Mechanics* (Courier, Chelmsford, 1938).
- [29] D. G. Luchinsky, P. V. E. McClintock, and M. I. Dykman, Analogue studies of nonlinear systems, *Rep. Prog. Phys.* **61**, 889 (1998).
- [30] K.-H. Chiang, C.-L. Lee, P.-Y. Lai, and Y.-F. Chen, Electrical autonomous Brownian gyrator, *Phys. Rev. E* **96**, 032123 (2017).
- [31] J. C. Neu, *Training Manual on Transport and Fluids* (American Mathematical Society, Providence, 2009).
- [32] J. C. Neu, *Singular Perturbation in the Physical Sciences* (American Mathematical Society, Providence, 2015).
- [33] J. C. Neu and S. W. Teitworth (unpublished).
- [34] L. C. Evans, *Partial Differential Equations* (American Mathematical Society, Providence, 2010).
- [35] P. H. Dannenberg, J. C. Neu, and S. W. Teitworth, Steering Most Probable Escape Paths by Varying Relative Noise Intensities, *Phys. Rev. Lett.* **113**, 020601 (2014).